INTERNATIONAL JOURNAL FOR NUMERICAL METHODS IN FLUIDS
Int. J. Numer. Meth. Fluids 2008; **56**:143–165
Published online 22 May 2007 in Wiley InterScience (www.interscience.wiley.com). DOI: 10.1002/fld.1518

Correlations of flow maldistribution parameters in an air cooled heat exchanger

M. A. Habib[1,*,†,‡], R. Ben-Mansour[1,§], S. A. M. Said[1,‡], J. J. Al-Bagawi[2,¶] and K. M. Al-Mansour[2,‖]

[1]*Mechanical Engineering Department, King Fahd University of Petroleum & Minerals, Dhahran 31261, Saudi Arabia*
[2]*Saudi Aramco, P.O. Box 5000, Dhahran 31311, Saudi Arabia*

SUMMARY

The present paper provides correlations of flow maldistribution parameters in air-cooled heat exchangers. The flow field in the inlet header was obtained through the numerical solution of the governing partial differential equations including the conservation equations of mass and momentum in addition to the equations of the turbulence model. The results were obtained for different number of nozzles of 2–4, different inlet flow velocities of 1–2.5 m/s and different nozzle geometries in addition to incorporation of a second header. The results are presented in terms of mass flow rate distributions in the tubes of the heat exchanger and their standard deviations. The results indicate that the inlet flow velocity has insignificant influence on maldistribution while the nozzle geometry shape has a slight effect. Also, the results indicate that reducing the nozzle diameter results in an increase in the flow maldistribution. A 25% increase is obtained in the standard deviation as a result of decreasing the diameter by 25%. Increasing the number of nozzles has a significant influence on the maldistribution. A reduction of 62.5% in the standard deviation of the mass flow rate inside the tubes is achieved by increasing the number of nozzles from 2 to 4. The results indicate that incorporating a second header results in a significant reduction in the flow maldistribution. A 50% decrease in the standard deviation is achieved as a result of incorporation of a second header of seven holes. It is also found that the hole-diameter distribution at the exit of the second header has a slight influence on the flow maldistribution. Correlations of the flow maldistribution in terms of the investigated parameters are presented. Copyright © 2007 John Wiley & Sons, Ltd.

Received 1 May 2006; Revised 18 March 2007; Accepted 26 March 2007

KEY WORDS: flow maldistribution; heat exchanger; correlations

*Correspondence to: M. A. Habib, Mechanical Engineering Department, King Fahd University of Petroleum & Minerals, Dhahran 31261, Saudi Arabia.
†E-mail: mahabib@kfupm.edu.sa
‡Professor.
§Assistant professor.
¶Coordinator of Professional Engineering Development Division.
‖Engineer, Consulting Services Department.

1. INTRODUCTION

The air-cooled heat exchangers are normally designed with the assumption that the fluid is uniformly divided among all the parallel tube passages. In practice, however, the design of the exchanger, the heat-transfer process and the operation of the external system may create high-flow maldistribution. The performance deterioration of air-cooled heat exchangers due to flow maldistribution may be serious. Such flow maldistribution from the main channel (header) to the branches can cause serious deterioration of the thermal performance of the heat exchanger. The flow distribution mechanism of the header and the calculation procedure for the design needs to be studied. The objective is to obtain a uniform flow distribution in cross-flow tubes so as to achieve uniform cooling throughout the heat exchanger. While heat exchanger design typically focuses on surface area requirements, the fluid-flow patterns within the tubes can be of equal importance. One optimization target is the equal distribution of flow into each tube within the bundle; in an unmodified heat exchanger, this rarely happens. The main objective of the present study is to develop guidelines for reducing flow maldistribution in air-cooled heat exchangers utilizing single-phase flows.

A general overview of maldistribution of flow [1] provided a brief summary of the panel discussion [2] on the effect of maldistribution of flow on the performance of heat-transfer equipment. It was reported that thermal performance deterioration in single-phase flows heat exchangers can be reduced by the use of good engineering judgment and design practice and there is a need for continued research in the area of two-phase flows maldistribution. The authors also report that there appears to be a need for continued validation of the variety of numerical/computational and experimental technique being developed, to assess local and overall effects of flow maldistribution on equipment. A method for predicting dynamic performances of parallel and counterflow heat exchangers subject to arbitrary temperature variations and step flow disturbances was developed [3]. The study included the effect of flow maldistribution and the influence of heat capacities of both fluids. Experiments were carried out on a heat exchanger to examine the feasibility of this method. The effects of air flow non-uniformity on the transfer performance of refrigerant evaporators were investigated by Timoney and Foley [4]. A single component traversing LDA system was used to determine local mean velocities and turbulence levels. Contrary to expectations, increases in heat-transfer as well as overall heat-transfer coefficients were recorded as air flow non-uniformities were artificially introduced, whilst a constant mean air velocity was maintained.

The transient behaviour of two welded plate heat exchangers was experimentally investigated by Das *et al.* [5] for identical construction but different numbers of plates under different operating conditions. The temperature response on both sides following a step change in inlet temperature on one side has been compared to a mathematical model that takes into account the effects of flow maldistribution within the channels and between channels by introducing a dispersion term in the energy equation. The model was validated by the experiments. It was found that the dispersion model gives a better simulation than the conventional plug-flow model. From the experiments the effects of number of transfer units (NTU), heat-capacity rate ratio, and number of plates were also determined. A dynamic simulation algorithm of multipass cross-flow heat exchangers with arbitrary rows per pass was proposed [6]. Heat capacities of both fluids and of the core wall as well as conduction resistance of the wall are taken into account. The effect of the possible tube-side flow maldistribution was described with the dispersed plug-flow model. Transient responses to arbitrary disturbances of inlet temperatures of both fluids were obtained. The thermal performance reduction in

DOI: 10.1002/fld

air-cooled heat exchangers due to non-uniform flow and temperature distributions was investigated [7]. The differences in performance characteristics of individual tube rows were also considered. The results show that non-uniform air velocity distribution to a tube row leaves the row with a distorted temperature profile. The temperature non-uniformity was found to increase as the air passes through subsequent tube rows. Velocity distributions were measured on air-cooled heat exchanger models and were used to determine the extent to which air flow maldistribution reduced exchanger performance. It was found that maldistribution occurring in well-designed air-cooled heat exchangers reduces the thermal performance by only a few per cent. In their earlier work, the effects of inlet fluid-flow non-uniformity on thermal performance and pressure drops in cross-flow plate–fin compact heat exchangers were investigated [8]. The analysis accounted for the effects of two-dimensional non-uniform inlet fluid-flow distribution on both hot and cold fluid sides. The analysis was carried out using a finite-element model. A mathematical equation was developed to generate different types of fluid-flow maldistribution models considering the possible deviations in fluid-flow. These fluid-flow maldistribution models were used to calculate the exchanger effectiveness and its deterioration due to flow non-uniformity for an entire range of design and operating conditions. In addition to thermal analysis, the pressure drops and their variations were also calculated for these models. It was found that the performance deteriorations and variation in pressure drops are quite significant in some typical applications due to fluid-flow non-uniformity.

Different models of plate and cross-flow heat exchangers that take into account flow maldistribution effects were described [9–11]. The effect of flow maldistribution on the performance of a laminar, counterflow, high-effectiveness heat exchanger has been analysed and quantified [12]. To correct the uneven heat-transfer distribution from the maldistributed mass flow in one, fins were connected in the other passage (screen mesh). A heat-transfer model was developed for both passages and a parametric study was conducted to present the effect of adding thermal paths to correct the uneven heat-transfer. Various types of flow maldistribution in heat exchangers were reviewed by Mueller and Chiou [13]. The effect of maldistribution on the heat exchanger performance as well as the causes of these maldistributions was investigated. The authors discussed in detail the mechanically, self-induced and two-phase flow maldistributions. They concluded that the most important factor affecting heat-transfer performance is the effect of flow maldistribution on the average effective temperature difference and that variation of coefficient is a minor factor. The effects of several types and patterns of maldistribution on the thermal performance of heat exchangers were investigated [14]. The effect of these maldistributions on the thermal performance of the exchanger was found to depend on the degree of each maldistribution and its source. Source includes design, heat-transfer process and operation of the external system. It was reported that there is a lack of concern over maldistribution due directly to relatively small reduction in thermal performance for exchangers with turbulent flow and small NTU. It was concluded [14] that the significance of maldistribution depends on how performance is evaluated. If a heat-transfer coefficient is to be calculated for comparison with other data and/or correlations, then a much greater error occurs because the maldistribution distorts the effective temperature difference. Secondary effects of maldistribution resulting from temperature distributions in the exchanger may result in significant stress problems. The effect of flow non-uniformity on the performance of heat exchangers was presented by Lalot *et al.* [15]. The investigation was based on the study of gross flow maldistribution in an experimental electrical heater. The study of the flow distribution in a particular heater shows that reverse flows may occur for poor inlet header design. A procedure was suggested to homogenize the flow distribution and a simple law to calculate, with good accuracy, the velocity ratio (ratio of the highest velocity in the tubes to the lowest velocity). It was

DOI: 10.1002/fld

shown that gross flow maldistribution leads to a loss of effectiveness of about 7% for condensers and counterflow heat exchangers, and up to 25% for cross-flow exchangers, for velocity ratios up to 15.

An analysis of a cross-flow plate–fin compact heat exchanger was carried out [16] using a finite-element method. The analysis accounts for the combined effect of two-dimensional longitudinal heat conduction through the exchanger wall and non-uniform inlet fluid-flow distribution on both hot and cold fluid sides. A factor for local flow non-uniformity was defined. As well, a parameter for measuring the degree of deformation was introduced. The exchanger effectiveness and its deterioration due to the combined effects of longitudinal heat conduction and flow non-uniformity were calculated for various design and operating conditions of the exchanger. It was found that the performance deteriorations are quite significant in some typical applications due to the combined effects of wall longitudinal heat conduction and inlet fluid-flow non-uniformity on cross-flow plate–fin heat exchanger. The axial dispersion model proposed [17] was used to take flow maldistribution in plate–fin heat exchangers into account. The effect of the axial heat conduction in separating plates was considered. The governing equation system is solved by means of Laplace transform and numerical inverse transform algorithms. The investigation confirms that, for plate–fin heat exchangers of aluminium the effect of the lateral heat conduction resistance of fins can usually be neglected because of their high-fin efficiency.

The study [18] indicates the importance of considering the heat-transfer coefficient inside the channels as a function of flow rate through that particular channel. This eliminates the contradictory proposition of unequal flow rates but an equal heat-transfer coefficient. A wide range of parametric study have been presented, which brings out effects such as those of the heat-capacity rate ratio, flow configuration, number of channels and correlation of heat transfer. The analysis suggested a better method of heat-transfer data analysis for plate heat exchangers. The effect of flow maldistribution on the thermal performance of a single-pass plate heat exchanger was studied analytically [19]. The study considered the flow variation from channel to channel. The study results indicate that consideration of variable flow rate only in channels tends to underestimate the thermal performance of the heat exchanger and it is necessary to consider a variable heat-transfer coefficient inside the channels as a function of flow rate. The flow distribution performance in a plate–fin heat exchanger has been experimentally studied and the distribution performance of different distributors' inlet angles has been measured. The combined effects of the inlet angle and mass flow rate on flow maldistribution have been studied by Jiao *et al*. [20] and provide a useful tool for optimum design of plate–fin heat exchangers. Three types of header configuration have been designed and manufactured. Correlations of flow maldistribution parameters *versus* Reynolds number under different header configurations were presented. Three parameters of flow maldistribution were introduced to evaluate the flow maldistribution. These are based on either velocity distribution or dimensionless standard deviation. The correlation of the dimensionless flow maldistribution parameters and Reynolds number was obtained under different header configurations. The ratio of the maximum flow velocity and the minimum flow velocity drops from 2.08–2.81 to 1.2–1.4 for various Reynolds numbers.

The effect of flow maldistribution on the thermal performance of a three-fluid cross-flow heat exchanger has been investigated numerically by Yuan [21]. The study considers four modes of flow non-uniformity arrangement by using three-flow maldistribution models. Local flow non-uniformity factors defined as the local flow rate over average mass flow and deterioration factor due to flow maldistribution were considered to evaluate influence of maldistribution. Effectiveness

DOI: 10.1002/fld

at different flow modes was presented. The study [21] discussed the deterioration or promotion due to the flow maldistribution in the heat exchanger. The results indicated that there is a best one in choice between the four maldistribution modes and the best flow maldistribution mode promotes the thermal performance of a three-fluid cross-flow heat exchanger when NTU and heat-capacity rate ratios are large.

The previous work is mainly related to the influence of flow maldistribution on the performance of heat exchangers but does not provide any focused work on the procedures that can be followed to improve the flow distribution inside air-cooled heat exchangers. Therefore, the present work is aimed at investigating the parameters influencing the flow maldistribution in air-cooled heat exchangers.

2. PROBLEM AND MATHEMATICAL FORMULATION

2.1. The flow domain

The calculations were performed inside the inlet header of the heat exchanger and the tubes of the tube sheet. Figure 1 shows the geometry of the header. The tube sheet has 32 tubes of diameter 25.65 mm distributed on one line as shown in the figure. Flow enters at the entrance section of the nozzles of the heat exchanger header. Abrupt expansion occurs at the nozzle exit section and the inlet to the header. The fluid then flows towards the tube sheet (Figure 1). Due to symmetry, only half of the tubes were considered in the numerical simulation. The fluid that is used as the working fluid is hydrocarbon oil having a density of $645.6\,\mathrm{kg/m^3}$ and a viscosity of $2.32\,\mathrm{Ns/m^2}$ at 139°C. For the base case, the mass flow rate is 12.27 kg/s and the inlet velocity is 1.429 m/s.

2.2. The calculation procedure

The conservation equations for mass and momentum were solved to predict the flow pattern of the flow. Since the flow is turbulent, additional transport equations for the turbulence model were also solved. The time-averaged governing equations of three-dimensional turbulent flow can be found in many references [22, 23] and can be presented as follows.

Mass conservation:

The steady-state time-averaged equation for conservation of mass can be written as

$$\frac{\partial}{\partial x_j}(\rho \overline{U}_j) = 0 \tag{1}$$

Momentum conservation:

The steady-state time-averaged equation for the conservation of momentum in the i direction can be expressed as

$$\frac{\partial}{\partial x_j}(\rho \overline{U}_i \overline{U}_j) + \frac{\partial}{\partial x_j}(\rho \overline{u_i u_j}) = -\frac{\partial p}{\partial x_i} + \frac{\partial}{\partial x_j}\left(\mu \frac{\partial U_i}{\partial x_j}\right) \tag{2}$$

DOI: 10.1002/fld

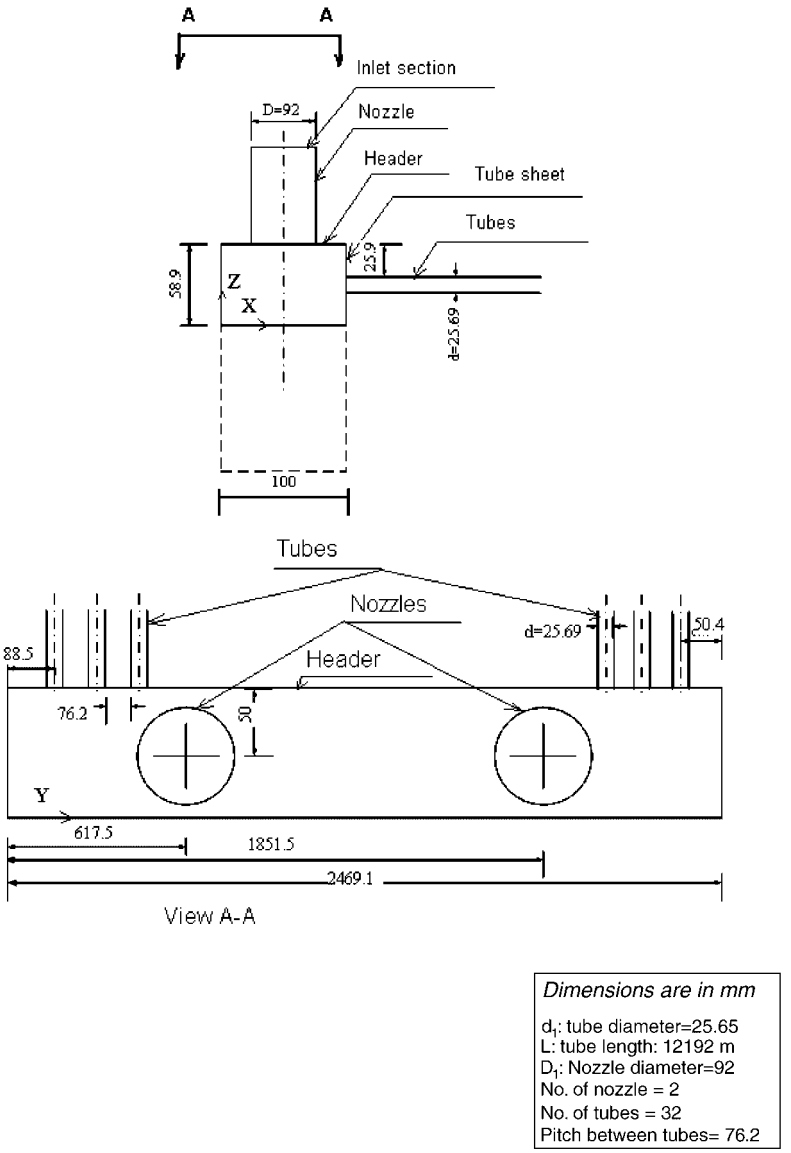

Figure 1. The geometry of the header.

where p is the static pressure. The stress tensor $\rho\overline{u_i u_j}$ is given by

$$-\rho\overline{u_i u_j} = \left[\mu_{\text{eff}}\left(\frac{\partial \overline{U}_i}{\partial x_j} + \frac{\partial \overline{U}_j}{\partial x_j}\right)\right] - \frac{2}{3}\rho k \delta_{ij} \tag{3}$$

DOI: 10.1002/fld

where δ_{ij} is the Kronecker delta which is equal to 1 for $i = j$ and equals 0 for $i \neq j$ and $\mu_{\text{eff}} = \mu_t + \mu$ is the effective viscosity. The turbulent viscosity, μ_t, is calculated using the high-Reynolds number form as

$$\mu_t = \rho C_\mu \frac{k^2}{\varepsilon} \tag{4}$$

with $C_\mu = 0.0845$. The value of C_μ is derived using the mathematical model 'renormalization group' [24] to accurately describe the variation of turbulent transport with effective Reynolds number, thus, providing better results for near-wall flows. The value of C_μ used in the present study is therefore different from the value 0.09 used for high-Reynolds number. k and ε are the kinetic energy of turbulence and its dissipation rate. These are obtained by solving their conservation equations [25, 26] as given below.

The kinetic energy of turbulence:

$$\frac{\partial}{\partial x_j}(\rho \overline{U}_j k) = \frac{\partial}{\partial x_j}\left(\frac{\mu_{\text{eff}}}{\sigma_k}\frac{\partial k}{\partial x_i}\right) + G_k - \rho\varepsilon \tag{5}$$

The rate of dissipation of the kinetic energy of turbulence:

$$\frac{\partial}{\partial x_j}(\rho \overline{U}_j \varepsilon) = \frac{\partial}{\partial x_i}\left(\frac{\mu_{\text{eff}}}{\sigma_\varepsilon}\frac{\partial \varepsilon}{\partial x_i}\right) + C_{\varepsilon 1} G_k \frac{\varepsilon}{k} - C_{\varepsilon 3}\rho\frac{\varepsilon^2}{k} \tag{6}$$

where G_k represents the generation of turbulent kinetic energy due to the mean velocity gradients and is given by

$$G_k = -\rho \overline{u_i u_j}\frac{\partial \overline{U}_j}{\partial x_i} \tag{7}$$

The quantities σ_k and σ_ε are the effective Prandtl numbers for k and ε, respectively, and $C_{\varepsilon 3}$ is given as a function of the term k/ε and, therefore, the model is responsive to the effects of rapid strain and streamline curvature and is suitable for the present calculations. Thus, $C_{\varepsilon 3}$ is expressed [26] as

$$C_{\varepsilon 3} = C_{\varepsilon 2} + \frac{C_\mu \rho \eta^3 (1-\eta)/\eta_0}{1 + \beta\eta^3}$$

with $\eta = Sk/\varepsilon$, $\eta_0 = 4.38$, $\beta = 0.012$. S being a scalar measure of the deformation tensor given by $S = \sqrt{2\omega_{ij}\omega_{ij}}$, where $\omega_{ij} = 0.5(\partial u_j/\partial x_i - \partial u_i/\partial x_j)$. The model constants $C_{\varepsilon 1}$ and $C_{\varepsilon 2}$ have the values; $C_{\varepsilon 1} = 1.42$ and $C_{\varepsilon 2} = 1.68$.

The wall functions establish the link between the field variables at the near-wall cells and the corresponding quantities at the wall. These are based on the assumptions introduced [27] and have been most widely used for industrial flow modelling [22].

Boundary conditions:

The velocity distribution at the nozzle inlet section is considered to be uniform with the velocity in the direction of the axis of the nozzle. The present calculations were conducted for isothermal flow where the fluid density and viscosity remain constant throughout the flow field.

Kinetic energy and its dissipation rate are assigned through a specified value of $\sqrt{k/\overline{U}^2} = 0.1$ and a length scale proportional to the diameter of the header inlet nozzle. These values are suitable for fully developed flow expected at the inlet to the header. For such flows, the turbulence intensity

DOI: 10.1002/fld

is in the range of 5–10%. The boundary condition applied at the exit section (the exit of the heat exchanger tubes) is that of a given pressure. At the wall boundaries, all velocity components are set to zero and kinetic energy of turbulence and its dissipation rate are determined from the equations of the turbulence model.

3. NUMERICAL SCHEME AND SOLUTION PROCEDURE

The conservation equations were solved simultaneously over a typical volume that is formed by division of the flow field into a number of control volumes, to yield the solution. Calculations are

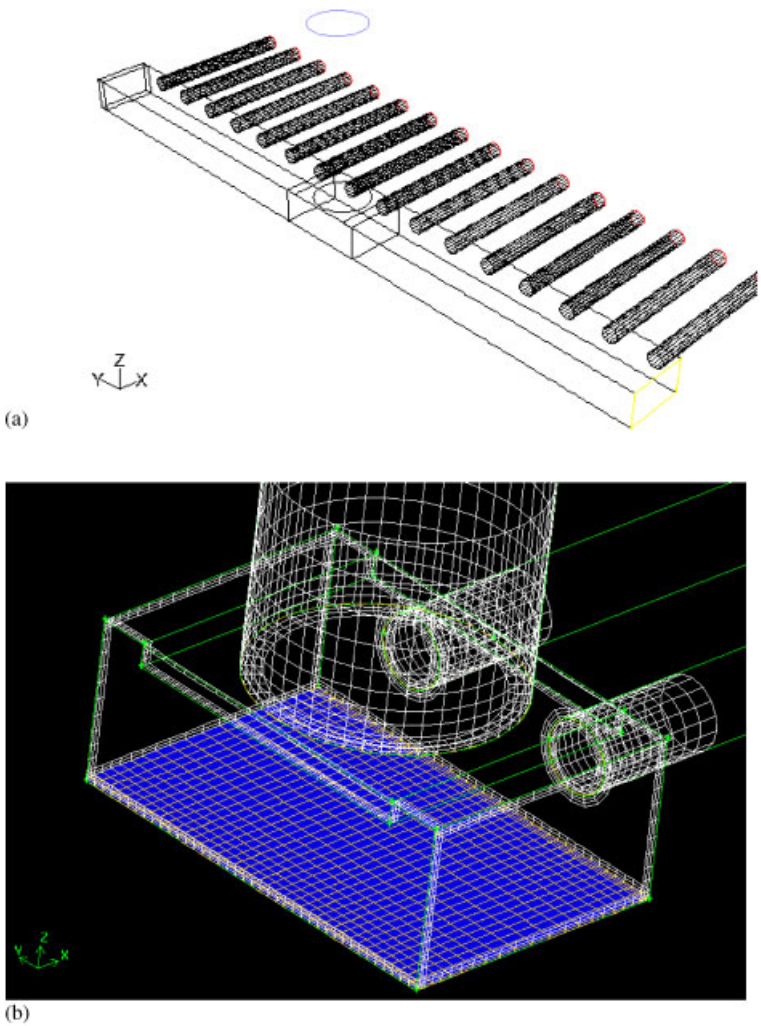

Figure 2. Flow domain and grid distribution in header, nozzle and tubes: (a) the flow domain including nozzle, header and tubes and (b) the grid distribution in header, nozzle and tubes.

DOI: 10.1002/fld

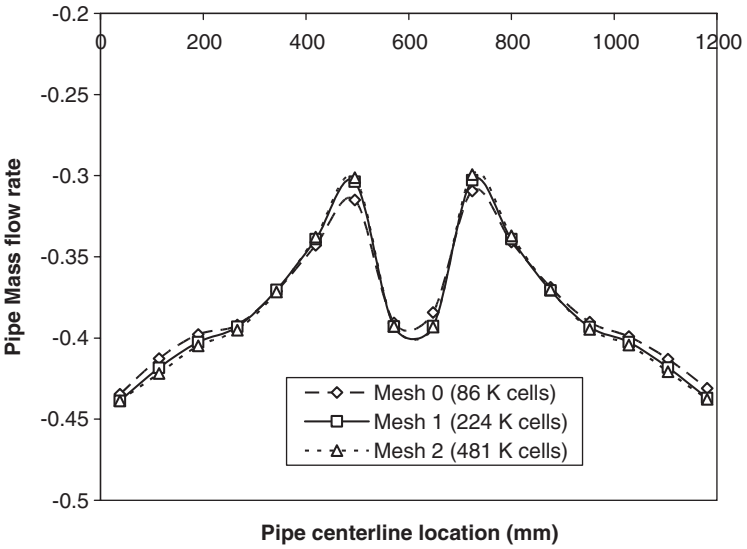

Figure 3. Grid-independence test.

performed with at least 224 000 elements considering fine elements in the section of the header close to the inlet of heat exchanger tubes. Structured mesh was used with concentration of grids near walls and in the vicinity of regions of high-velocity gradients. The flow domain and grid distribution in header, nozzle and tubes are shown in Figure 2. In order to provide flexibility of nozzle location and diameters, the header was divided into segments. The grid distributions of all segments are constructed with refined mesh close to the solid walls and at the entrance of the tubes. It is worth noting here that structured grids have been used (except for the three-dimensional intersection between the nozzle and header) in order to have the best computational efficiency. This task has taken a lot of care and effort to obtain the structured grid. The structured grid has been designed semi-manually after many trials. This allowed the placement of grid boundary layers at all the walls of the header, nozzle and pipes. It was believed that this effort was required in order to capture the correct flow and pressure field as well as the vena-contracta for all the 16 pipes in the base geometry. In order to establish grid independence, three different grids were used. The coarser grid had 86 000 cells (Mesh0), the medium size grid had 224 000 cells (Mesh1) and a finer grid had 481 000 cells (Mesh2). Since one of the main goals of the study is to investigate the mass flow rate distribution, the comparison between the grids is based on the mass flow rates through the 16 pipes. The results are shown in Figure 3. The difference in mass flow rates between Mesh1 and Mesh2 varied between $\pm 0.01\%$ which is a very tight tolerance. Hence, Mesh1 has been adopted for the rest of the study. In the above runs and the rest of the study, the simulations were executed until the mass error, velocity errors as well and k and ε errors as measured by the residuals of their equations, being summed for all the grid nodes, were all below 10^{-6}. The procedure used a hybrid (upwind central) differencing scheme in solving all the governing partial differential equations. The discretized equations were solved using an iterative method [28]. The SIMPLE algorithm was used as the pressure velocity coupling for solving the mass conservation and pressure field. In this scheme, the solution of the momentum equations is followed by solving

DOI: 10.1002/fld

the pressure correction equation. CFD packages Fluent 6.1.22 [29] were used for performing the present calculations in the present work.

4. RESULTS

The features of the flow inside the header and tubes are presented in Figures 4 and 5. Figure 4 presents the pathlines of the flow field inside the header and tubes. It indicates flow separation at the inlet of the tubes. The size and strength of the recirculated flow region depend significantly on the location of the tube. The contours of the velocity magnitude are exhibited in Figure 5 and indicate high velocity values at the nozzle exit and at the inlet of the tubes close to the nozzle and at the far end of the nozzle. Six parameters are considered in the present work. These are the inlet flow velocity, the nozzle diameter, the number of nozzles, the nozzle geometry and the incorporation of a second header in addition to the number of passes. The results were obtained

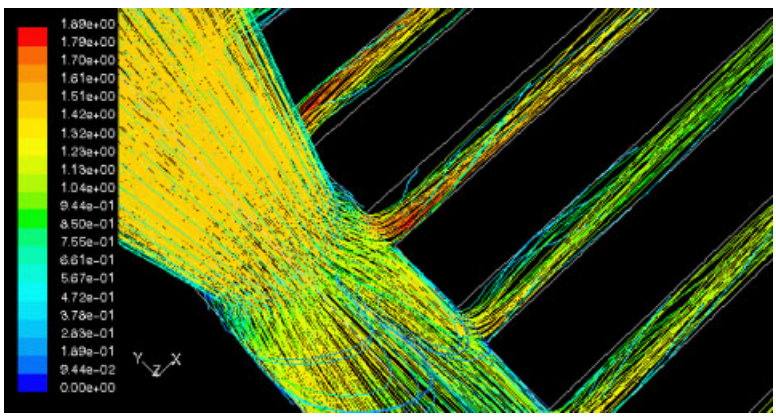

Figure 4. Pathlines of the flow field inside the header and tubes.

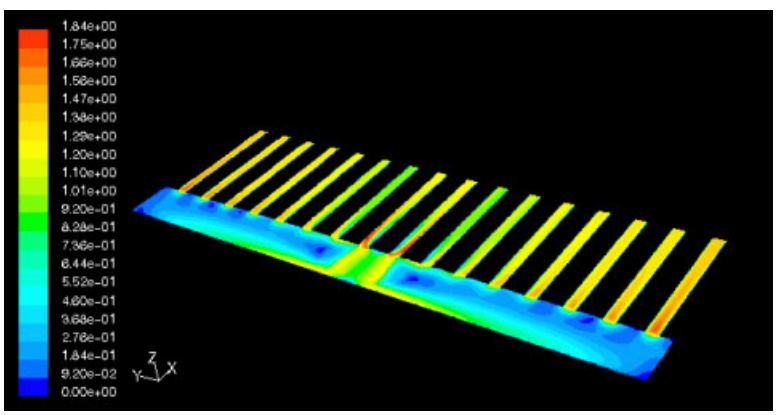

Figure 5. Velocity magnitude at section $z = 33$ mm s of the air-cooled heat exchanger.

DOI: 10.1002/fld

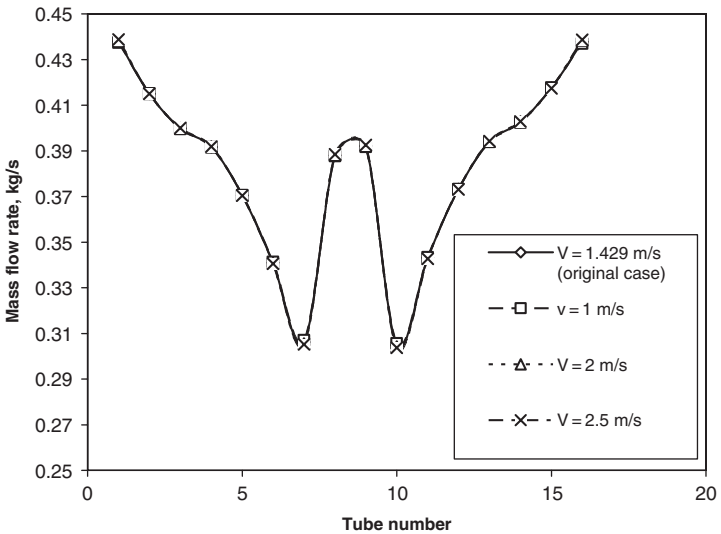

Figure 6. Distribution of mass flow rate among the tubes of the air-cooled heat exchanger at different values of inlet flow velocity.

for different number of nozzles of 3–4 in addition to the present geometry of two nozzles, different nozzle diameters of 69.0, 85.0 mm in addition to 92.0 of the original geometry, different inlet flow velocities of 1, 2 and 2.5 m/s in addition to 1.429 of the original case as well as incorporation of a second header. Second headers of three holes of $d = 56$ mm each and seven holes of 36.3 mm each were used. Hole patterns of (59.1, 49.24, 59.1) mm and (61.22, 43.73, 61.22) mm were used for the case of three holes. The flow maldistribution is evaluated through the presentation of the standard deviation (STD) in the mass flow rate distribution in the heat exchanger tubes as well as the static pressure distribution inside the main and return headers. The STD of a variable ϕ is given as

$$\mathrm{STD} = \sqrt{\left[\frac{1}{n-1}\sum_{i=1}^{n}\left(\frac{\dot{m}_i}{\dot{m}_{\mathrm{avg}}} - 1\right)^2\right]} \tag{8}$$

where n is the number of tubes, $\dot{m}_i$ is the mass flow rate in the tube number i and $\dot{m}_{\mathrm{avg}}$ is the average value of the mass flow rate. The influence of the different parameters on the mass flow distributions and their STDs is given in the following.

The distribution of the mass flow rate in the tubes is shown in Figure 6 for different values of inlet flow velocity in the range of 1–2.5 m/s. The values of the mass flow rate in each tube are calculated from the integration of the flow velocity inside each tube. The figure indicates that the inlet velocity has a negligible influence on the maldistribution. The STDs are shown in Figure 7 and indicate a maximum difference of 2.5%. The influence of the nozzle diameter on the mass flow rate distribution is shown in Figure 8. The considered diameters are 69.0, 80.5 and 92.0 mm. The figure indicates that reducing the diameter results in an increase in the flow maldistribution. The results of the influence of the nozzle diameter on the STDs in the mass flow rates in the tubes

DOI: 10.1002/fld

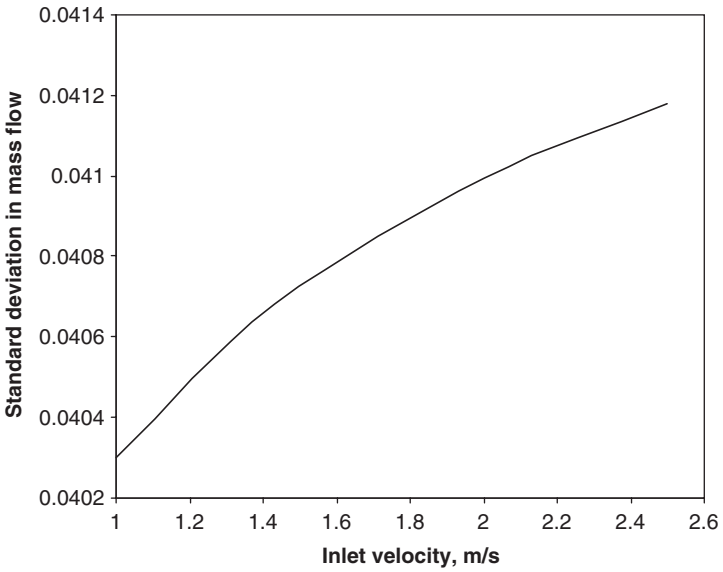

Figure 7. Influence of the inlet flow velocity on the standard deviation of the mass flow rate distribution.

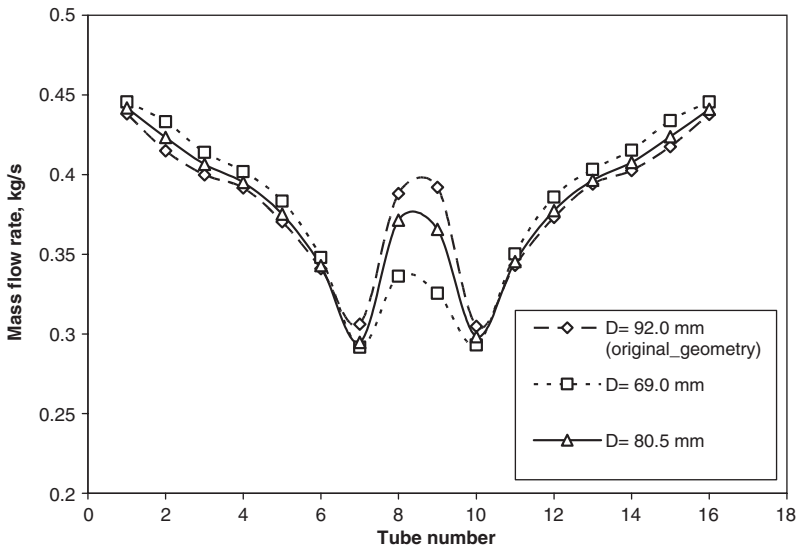

Figure 8. Distribution of mass flow rate among the tubes of the air-cooled heat exchanger at different values of nozzle diameter.

of the inlet header are shown in Figure 9. It is indicated that decreasing the diameter by 25% results in 25% increase in the standard deviation. The flow maldistribution is greatly influenced

DOI: 10.1002/fld

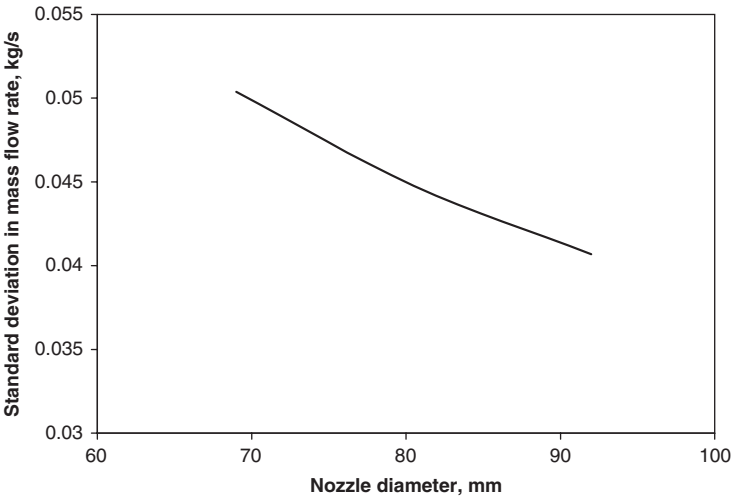

Figure 9. Influence of the nozzle diameter on the standard deviation of the mass flow rate.

by the difference in pressure inside the header and the tubes. As the area increases, the pressure at exit increases and the pressure inside the header increases in comparison of the pressure inside the tubes, thus, resulting in more uniform flow inside the tubes.

The influence of nozzle geometry on the mass flow distribution and its STD is shown in Figures 10 and 11. Three different nozzle geometries are considered in the present study. The first is the original geometry in which the nozzle is having a cylindrical shape. The other two nozzle geometries are having elliptical cross section at their exit. The exit is an ellipse of diameters $a \times b$. The first elliptical geometry, A, has diameters $(a \times b)$ of 85.3×110.1 mm. The second elliptical geometry, B, has diameters $(a \times b)$ of 71.3×131.7 mm. The influence of the nozzle geometry on the distribution of the mass flow rate is shown in Figure 10. The figure indicates that increasing the diameter ratio of the nozzle cross section results in a decrease in the flow maldistribution. Twenty per cent decrease in the STD is shown in Figure 11 as a result of increasing the diameter ratio of the nozzle cross section from 1 to 1.85. The improvement in the flow distribution is attributed to the reduction in the velocity at exit of the nozzle and the corresponding resulting uniform static pressure distribution inside the header.

Figures 12 and 13 present the influence of the number of nozzles on the distribution of the mass flow rate inside the tube and its STD. The distribution of the mass flow rate in the tubes is shown in Figure 12 for different number of nozzles. It should be noted that the nozzles are equally spaced across the header. The figure indicates that increasing the number of nozzles has a significant influence on the maldistribution. Figure 13 presents the STD and indicates that a reduction of 62.5% in the STD is achieved by increasing the number of nozzles from 2 to 4. This is attributed to the resulting uniformity in the static pressure distributions as a result of increasing the number of nozzles.

The influence of incorporation of a second header on the flow distribution among the tubes was investigated. In order to provide a uniform flow distribution among the tubes, it is recommended to incorporate a second header between the nozzle and the current header. The objective is to provide a smooth transition from the nozzle to the main header. This provides a uniform pressure

DOI: 10.1002/fld

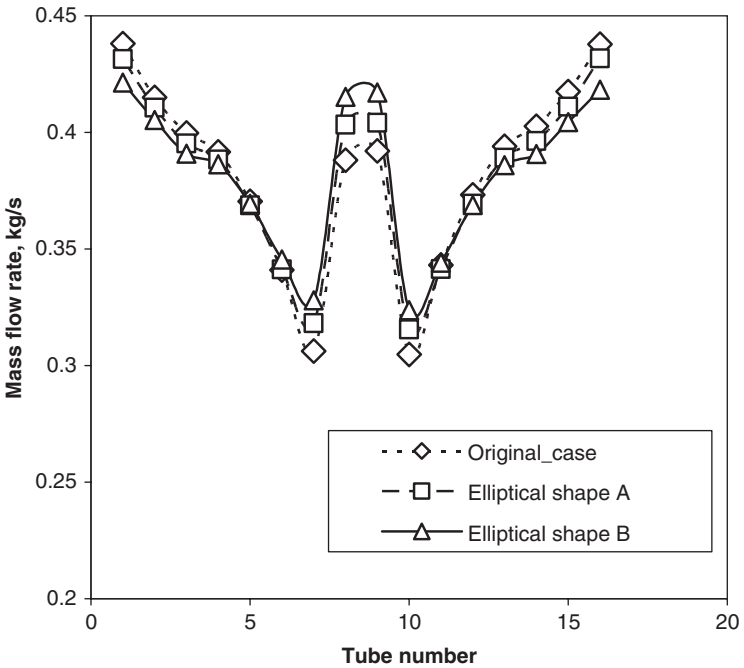

Figure 10. Distribution of mass flow rate among the tubes of the air-cooled heat exchanger at different nozzle geometries.

at inlet of the tubes. The second header, Figure 14 is half a cylinder having a diameter equal to the header width (100 mm). The second header is connected between the nozzles and the main header and is having a number of holes at its exit section. The number of holes at its exit is ranging from three holes of 56 mm diameter each to seven holes of 36.3 mm diameter each. The diameter of the holes in the case of three holes also has been changed from [59.1, 49.24, 59.1] mm to [61.22, 43.73, 61.22] mm to investigate the influence of the hole-diameter distribution in the second header on the mass flow rate distribution in the tubes. The influence of the number of holes on the mass flow rate is shown in Figures 15 and 16.

The influence of the number of holes of the second header on the mass flow rate is shown in Figure 15 and the influence of the number of holes on the STDs is shown in Figure 16. The figures indicate that incorporating a second heater results in a significant reduction in the flow maldistribution. Forty-five per cent decrease in the standard deviation is shown in Figure 16 as a result of incorporation of a second header of three holes. The improvement is attributed to the uniform distribution as a result of having more holes. This improvement is enhanced to 62.5% as the number of holes at the exit of the second header increases to seven holes. Similar conclusions were reported by Jiao *et al*. [20] for plate–fin heat exchangers. The present results were compared to the experimental results [30] of measured flow distributions in plate–fin heat exchanger. The comparison of the normalized STDs at different number of holes of the second header is presented in Figure 17 and indicates reasonable agreement.

The influence of the size of the holes in the second header on the mass flow rate is shown in Figure 18. The influence of the size of holes on the STD is shown in Figure 19. Three cases

DOI: 10.1002/fld

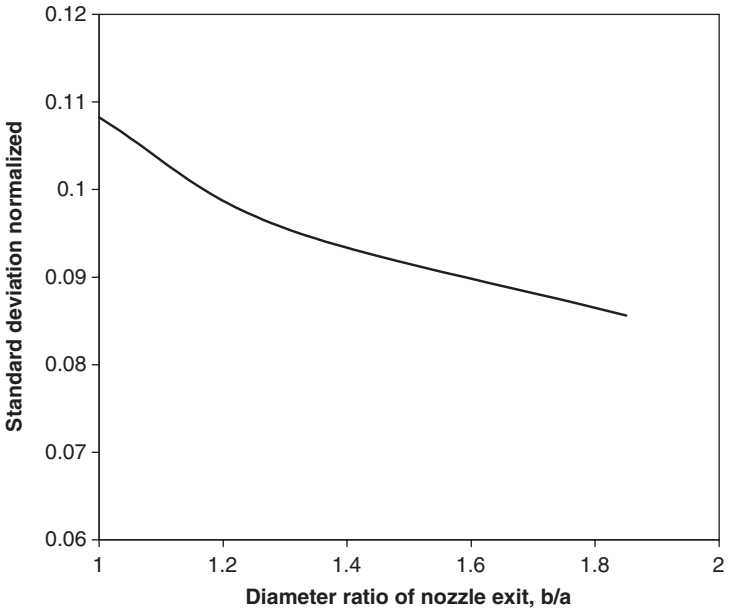

Figure 11. Influence of the nozzle geometry (diameter ratio of nozzle exit, b/a) on the standard deviation of the mass flow rate.

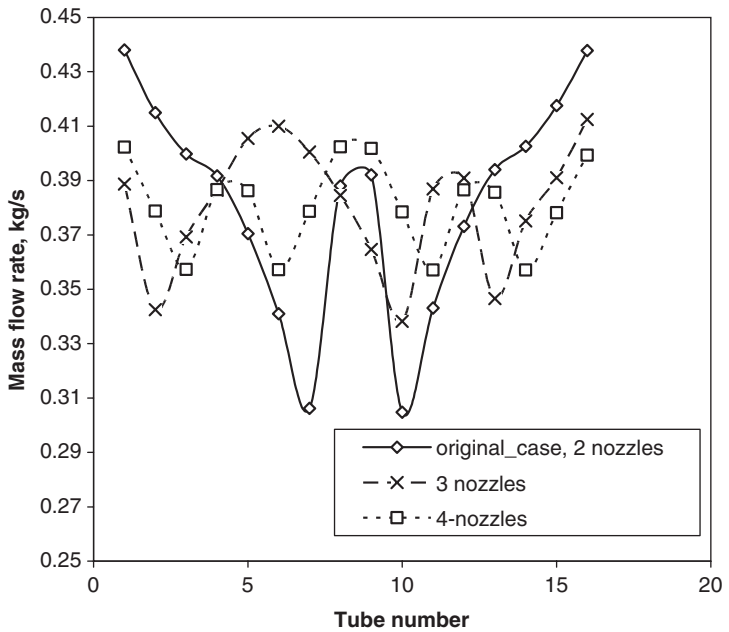

Figure 12. Distribution of mass flow rate among the tubes of the air-cooled heat exchanger for different number of nozzles.

DOI: 10.1002/fld

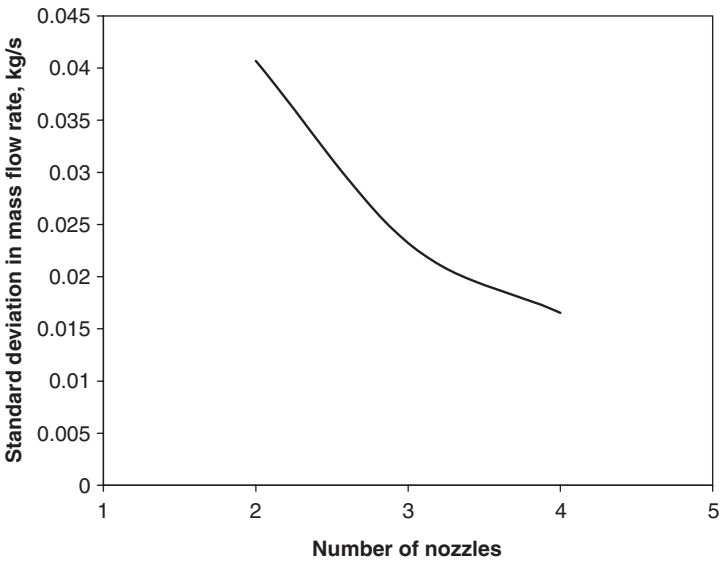

Figure 13. Influence of the number of nozzles on the standard deviation of the mass flow rate.

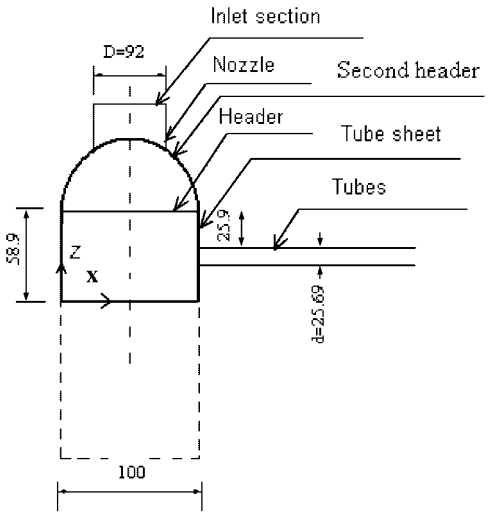

Figure 14. View indicating the location of the second header.

are considered. All of them are having three holes. The first case has hole-diameter pattern of pattern # 1 of [56, 56, 56] mm. The second case has pattern # 2 of [59.1, 49.24, 59.1] mm and the third case has pattern # 3 of [61.22, 43.73, 61.22] mm. The figures indicate that the hole-diameter pattern has a slight influence on the flow maldistribution. Three per cent variation in the STD is shown in Figure 19.

DOI: 10.1002/fld

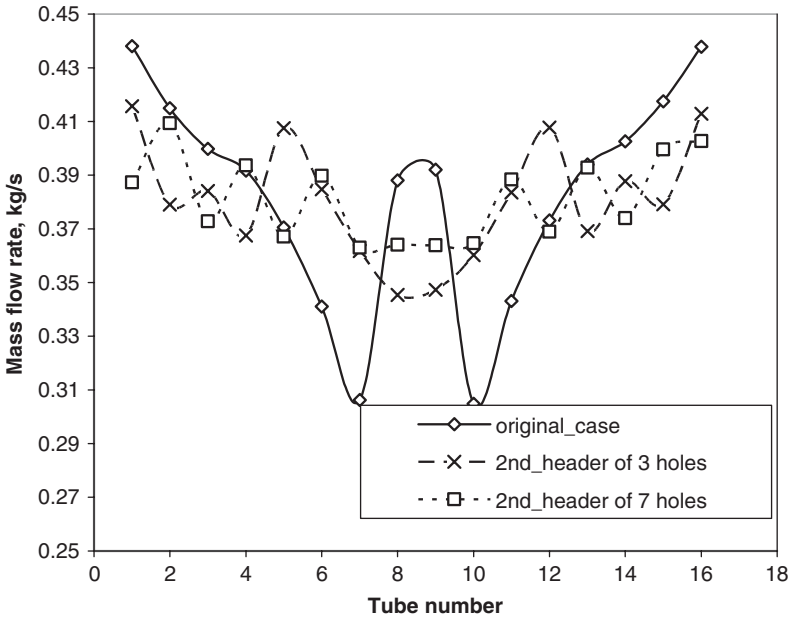

Figure 15. Distribution of mass flow rate among the tubes of the air-cooled heat exchanger at different number of holes in the second header.

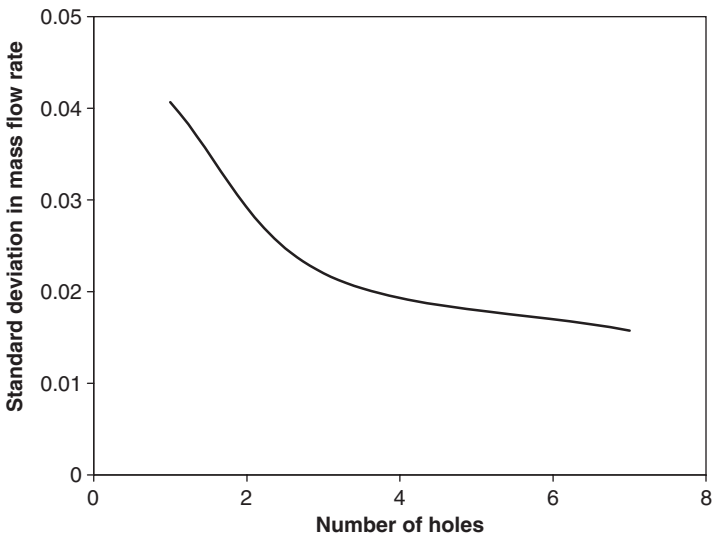

Figure 16. Influence of the number of holes of a second header on the standard deviation of the mass flow rate.

DOI: 10.1002/fld

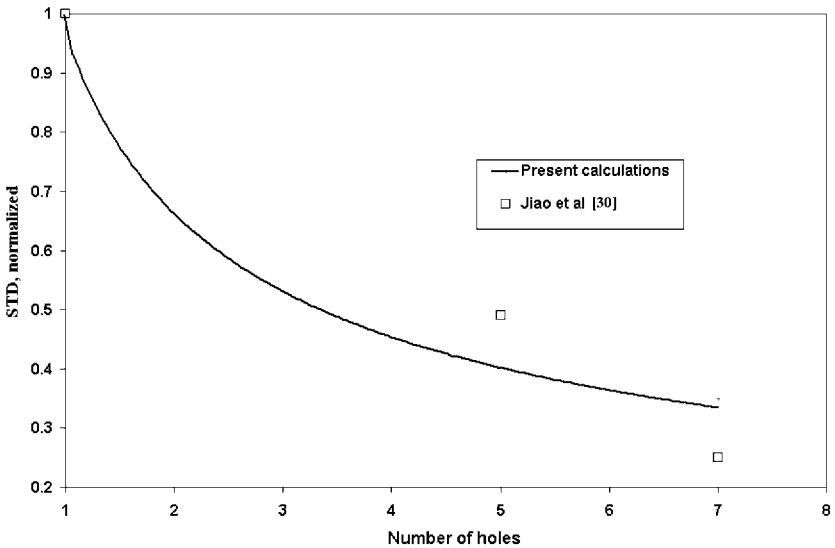

Figure 17. Comparison of the present calculations of STD variations with the number of holes in the second header and experiments of Jiao *et al*. [30].

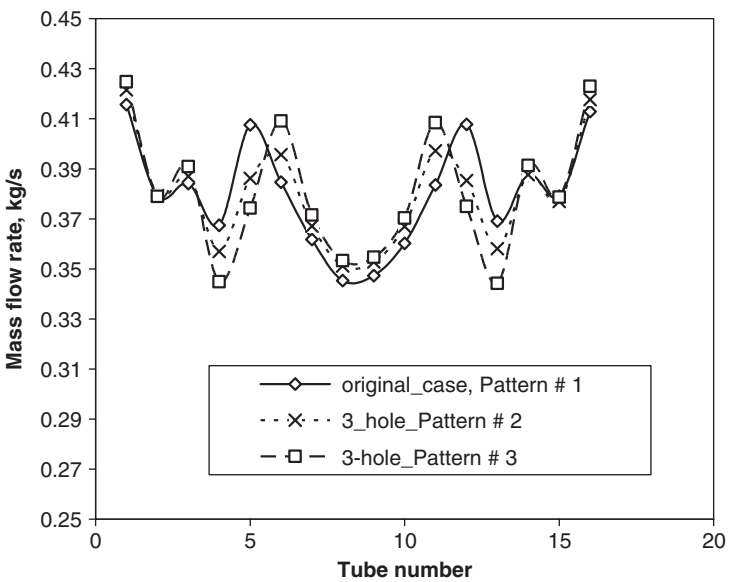

Figure 18. Influence of second header hole diameter (pattern #) on the distribution of mass flow rate among the tubes of the air-cooled heat exchanger.

DOI: 10.1002/fld

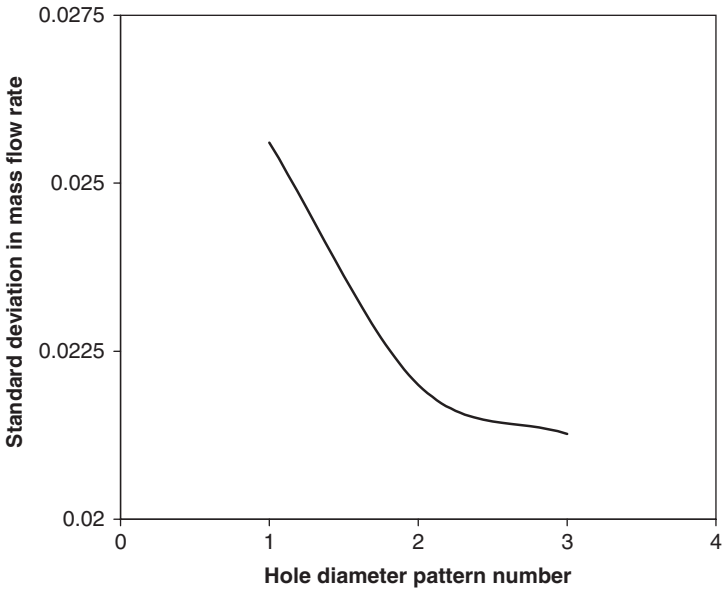

Figure 19. Influence of the hole diameter (pattern #) of the second header on the standard deviation of the mass flow rate.

5. CORRELATIONS OF FLOW MALDISTRIBUTION

Correlations of the influence of the different parameters on the flow maldistribution in the tubes of the air-cooled heat exchangers are developed. The magnitude of the flow maldistribution in the tubes of air-cooled heat exchangers is expressed in terms of the intensity of mass flow rate variation (I) and the maximum mass flow rate variation (γ). The intensity, I, is the normalized per cent standard of the deviation in the mass flow rate in the tubes. The intensity, I, is expressed by the following expression:

$$I = \frac{\text{STD}}{\dot{m}_{\text{av}}} * 100 \tag{9}$$

where $\dot{m}_{\text{av}}$ is the average of the mass flow rates inside the heat exchanger tubes. STD is the standard deviation in the mass flow rate distribution in the tubes and is given by Equation (8). The maximum mass flow rate variation, γ, is the normalized per cent difference of the maximum and minimum flow rates inside the tubes

$$\gamma = \frac{\dot{m}_{\text{max}} - \dot{m}_{\text{min}}}{\dot{m}_{\text{av}}} * 100 \tag{10}$$

where $\dot{m}_{\text{max}}$ and $\dot{m}_{\text{min}}$ are the maximum and minimum mass flow rates in the tubes.

Based on the results of the study, correlations for reducing the flow maldistribution are developed. The correlations were conducted through the use of fitted formulae to the data of the intensity I and the mass flow variation γ as defined by Equations (9) and (10). The correlations for the intensity were obtained using Figures 7, 9, 11, 13 and 16. The correlations for γ were obtained using

DOI: 10.1002/fld

Figures 6, 8, 10, 12 and 15. The correlations were developed with a coefficient of determination ranging from 99.9 to 100%. The correlations pertain to the influence of number of nozzles, nozzle diameter, a second header, the nozzle geometry and the number of tube passes. The following correlations are to be considered in the design or modifications of air-cooled heat exchangers.

Influence of the number of nozzles: The influence of a number of nozzles on the magnitude of the flow maldistribution is correlated in terms of the ratio of the cross-sectional area of the nozzles to the total tubes cross-sectional area for a given nozzle cross-sectional area. The correlations are given as

$$I = 7.95/(A_r)^{1.3} \quad \text{For the range } 0.8 \leqslant A_r \leqslant 1.6 \tag{11}$$

$$\gamma = 25.2/(A_r)^{1.54} \quad \text{For the range } 0.8 \leqslant A_r \leqslant 1.6 \tag{12}$$

A_r is the ratio of the total cross-sectional area of inlet nozzles to the total cross-sectional area of the tubes defined as follows:

$$A_r = \frac{A_i}{A_0} \tag{13}$$

where A_i is the total cross-sectional area of inlet nozzles and A_0 is the total cross-sectional area of the tubes.

Influence of the nozzle diameter: The influence of the nozzle diameter on the magnitude of the flow maldistribution is correlated in terms of the ratio of the cross-sectional area of the nozzles to the total tubes cross-sectional area. The correlations are given as

$$I = 9.8/(A_r)^{0.37} \quad \text{For the range } 0.4 \leqslant A_r \leqslant 0.8 \tag{14}$$

$$\gamma = 38.7 + 14.5 * A_r - 23.9 * (A_r)^2 \quad \text{For the range } 0.4 \leqslant A_r \leqslant 0.8 \tag{15}$$

Influence of a second header: The second header is normally incorporated between the nozzles and the main header. The flow exiting the second header passes to the main header through a number of holes. The magnitude of the flow maldistribution is correlated in terms of the number of holes (N) between the two headers. The correlations are given as

$$I = 10.4/(N)^{0.49} \quad \text{For the range } 1 \leqslant N \leqslant 7 \tag{16}$$

$$\gamma = 34.5/(N)^{0.54} \quad \text{For the range } 1 \leqslant N \leqslant 7 \tag{17}$$

Influence of the nozzle geometry: The use of nozzles of elliptical (or elongated) shape results in significant reduction in the magnitude of the flow maldistribution compared to nozzles of cylindrical shape having the same cross-sectional area. The magnitude of the flow maldistribution is correlated in terms of the ratio of the diameters of the elliptical cross-sectional area of the nozzle. The correlations are given as

$$I = 18 - 9.7\alpha + 2.5\alpha^2 \quad \text{For the range } 1.0 \leqslant \alpha \leqslant 1.9 \tag{18}$$

$$\gamma = 66 - 40.9\alpha + 10.4\alpha^2 \quad \text{For the range } 1.0 \leqslant \alpha \leqslant 1.9 \tag{19}$$

where α is the ratio of the diameters of the elliptical cross-sectional area of the nozzle.

DOI: 10.1002/fld

6. CONCLUSIONS

The following conclusions are drawn from the results of the present study:

1. The inlet flow velocity has a negligible influence on the maldistribution.
2. The reduction in the nozzle diameter results in an increase in the flow maldistribution.
3. Increasing the number of nozzles has a significant influence on the maldistribution. A reduction of 62.5% in the flow STD of the mass flow distribution inside the heat exchanger tubes is achieved by increasing the number of nozzles from 2 to 4.
4. Using an elliptical nozzle cross section has shown to reduce the maldistribution. Increasing the diameter ratio of the nozzle cross section results in a decrease in the flow maldistribution.
5. Incorporating a second header results in a significant reduction in the flow maldistribution. 62.5% decrease in the standard deviation of the mass flow inside the tubes is achieved as a result of incorporation of a second header of seven holes.
6. The hole-diameter distribution of the second header has a slight influence on the flow maldistribution.

NOMENCLATURE

a, b	minimum and maximum diameters at exit of the elliptical nozzle
A_i	the total cross-sectional area of inlet nozzles
A_0	the total cross-sectional area of the tubes
A_r	the ratio of the total cross-sectional area of inlet nozzles to the total cross-sectional area of the tubes and is given by $A_r = A_i/A_0$
$C_{\varepsilon 1}$	constant
$C_{\varepsilon 2}$	constant
C_μ	constant
d	hole diameter of the second header
D	nozzle diameter
G	generation of the turbulent kinetic energy
I	the intensity of mass flow rate variation
k	turbulent kinetic energy
$\dot{m}_{\text{avg}}$	the average value of the mass flow rate
$\dot{m}_i$	the mass flow rate in tube i
n	the number of tubes
N	number of holes in the second header
STD	standard deviation
$\overline{U}_j$	mean velocity
V	inlet flow velocity
x_j	coordinate

Greek symbols

α	the ratio of the diameters of the elliptical cross-sectional area of the nozzle and is given by $\alpha. = b/a$
γ	the maximum variation in the mass flow rate

DOI: 10.1002/fld

δ Kronecker delta
ε rate of dissipation of turbulent kinetic energy
μ viscosity
ρ density
σ effective Prandtl number

Subscripts

eff effective
max maximum value
min minimum value
t turbulent

Superscripts

$\cdot$ rate
— average value

ACKNOWLEDGEMENTS

The authors wish to acknowledge the support received from the Research Institute, King Fahd University of Petroleum & Minerals during this study.

REFERENCES

1. Kitto JB, Robertson JM. Effects of maldistribution of flow on heat-transfer equipment performance. *Journal of Heat Transfer Engineering* 1989; **10**(1):18–25.
2. Kitto JB, Robertson JM. *Maldistribution of Flow and its Effect on Heat Exchanger Performance*. American Society of Mechanical Engineers: New York, 1987.
3. Xuan Y, Roetzel W. Dynamics of shell-and-tube heat-exchangers to arbitrary temperature and step flow vibrations. *AICHE Journal* 1993; **39**(3):413–421.
4. Timoney DJ, Foley PJ. Some effects of air flow maldistribution on performance of a compact evaporator with R134A. *Heat Recovery Systems and CHP* 1994; **14**(5):517–523.
5. Das SK, Spang B, Roetzel W. Dynamic behavior of plate heat exchangers—experiments and modeling. *Journal of Heat Transfer* (ASME) 1995; **117**(4):859–864.
6. Xuan Y. Transient analysis of multipass cross-flow heat exchangers. *Heat and Mass Transfer* 1996; **31**(4):223–230.
7. Beiler MG, Kroger DG. Thermal performance reduction in air-cooled heat exchangers due to non-uniform flow and temperature distributions. *Heat Transfer Engineering* 1996; **17**(1):82–92.
8. Ranganayakulu C, Seetharamu KN, Sreevatsan KV. The effects of inlet fluid flow non-uniformity on thermal performance and pressure drops in crossflow plate–fin compact heat exchangers. *International Journal of Heat and Mass Transfer* 1997; **40**(1):27–38.
9. Luo X, Roetzel W. Theoretical investigation on cross-flow heat exchangers with axial dispersion in one fluid. *Revue Generale de Thermique* 1998; **37**(3):223–233.
10. Chen H, Cao C, Xu LL, Xiao TH, Jiang GL. Experimental velocity measurements and effect of flow maldistribution on predicted permeator performances. *Journal of Membrane Science* 1998; **139**(2):259–268.
11. Thonon B, Mercier P. Plate heat exchangers: ten years of research at GREThh.2. Sizing and flow maldistribution. *Revue Generale de Thermique* 1996; **35**(4):561–568.
12. Ratts EB. Investigation of flow maldistribution in a concentric-tube, counterflow, laminar heat exchanger. *Heat Transfer Engineering* 1998; **19**(3):65–75.
13. Mueller AC, Chiou JP. Review of various types of flow maldistribution in heat exchangers. *Journal of Heat Transfer Engineering* 1988; **9**(2):36–50.

DOI: 10.1002/fld

14. Mueller AC. Effect of some types of maldistribution on the performance of heat exchangers. *Journal of Heat Transfer Engineering* 1987; **8**(2):75–86.
15. Lalot S, Florent P, Lang SK, Bergles AE. Flow maldistribution in heat exchangers. *Applied Thermal Engineering* 1999; **19**(8):847–863.
16. Ranganayakulu C, Seetharamu KN. The combined effects of wall longitudinal heat conduction and inlet fluid flow maldistribution in crossflow plate–fin heat, exchangers. *Heat and Mass Transfer* 2000; **36**(3):247–256.
17. Luo X, Roetzel W. The single-blow transient testing technique for plate–fin heat exchangers. *International Journal of Heat and Mass Transfer* 2001; **44**(19):3745–3753.
18. Rao BP, Kumar PK, Das SK. Effect of flow distribution to the channels on the thermal performance of a plate heat exchanger. *Chemical Engineering and Processing* 2002; **41**(1):49–58.
19. Rao AJ, Zhang R, Jeong SA. Experimental investigation of header configuration on flow maldistribution in plate–fin heat exchanger. *Applied Thermal Engineering* 2003; **23**(10):1235–1246.
20. Jiao AJ, Li YZ, Chen CZ, Zhang R. Experimental investigation on fluid flow maldistribution in plate–fin heat exchangers. *Heat Transfer Engineering* 2003; **24**(4):25–31.
21. Yuan P. Effect of inlet flow maldistribution on the thermal performance of a three-fluid crossflow heat exchanger. *International Journal of Heat and Mass Transfer* 2003; **46**(20):3777–3787.
22. Habib MA, Attya AE, McEligot DM. Calculation of turbulent flow and heat transfer in channels with streamwise periodic flow. *ASME Journal of Turbomachinery* 1989; **110**:405–411.
23. Versteeg HK, Malalasekera W. *An Introduction to Computational Fluid Dynamics. The Finite Volume Method*. Longman: New York, 1995.
24. Choudhury D. Introduction to the renormalization group method and turbulence modeling. *Fluent Inc.*, *Technical Memorandum TM-107*, 1993.
25. Reynolds WC. Fundamentals of turbulence for turbulence modeling and simulation. Lecture Notes for Von Karman Institute. *Agard Report No. 755*, 1987.
26. Shih TH, Liou WW, Shabbir A, Zhu J. A new k–ε eddy–viscosity model for high Reynolds number turbulent flows—model development and validation. *Computers and Fluids* 1995; **24**(3):227–238.
27. Launder BE, Spalding DB. The numerical computation of turbulent flows. *Computer Methods in Applied Mechanics and Engineering* 1974; **3**:269–289.
28. Patankar SV. *Numerical Heat Transfer and Fluid Flow*. Hemisphere: Washington, DC, 1980.
29. Fluent Inc. *Fluent 6.1 User's Guide*. Fluent Inc.: Lebanon, NH, U.S.A., 2003.
30. Jiao A, Zhang R, Jeong S. Experimental investigation of header configuration on flow maldistribution in plate–fin heat exchanger. *Applied Thermal Engineering* 2003; **23**:1235–1246.

DOI: 10.1002/fld